

See discussions, stats, and author profiles for this publication at: <https://www.researchgate.net/publication/332822237>

Model reduction of structural biological networks by cycle removal

Conference Paper · May 2019

DOI: 10.1111/12.2519552

CITATIONS

0

READS

17

6 authors, including:



Amirhessam Tahmassebi

Florida State University

30 PUBLICATIONS 75 CITATIONS

[SEE PROFILE](#)



Behshad Mohebal

Florida State University

9 PUBLICATIONS 22 CITATIONS

[SEE PROFILE](#)



Philip Solimine

Florida State University

2 PUBLICATIONS 0 CITATIONS

[SEE PROFILE](#)



Katja Pinker

Medical University of Vienna

290 PUBLICATIONS 3,001 CITATIONS

[SEE PROFILE](#)

Some of the authors of this publication are also working on these related projects:



Grounding strategies for all-electric shipboard power systems [View project](#)



Intellectual Property Protection of high-level hardware descriptions [View project](#)

Model Reduction of Structural Biological Networks by Cycle Removal

Amirhessam Tahmassebi^{a,*}, Behshad Mohebbali^a, Philip Solimine^b, Uwe Meyer-Baese^c, Katja Pinker^{a,d,e}, and Anke Meyer-Baese^a

^aDepartment of Scientific Computing, Florida State University, Tallahassee, Florida, USA

^bDepartment of Economics, Florida State University, Tallahassee, Florida, USA

^cDepartment of Electrical and Computer Engineering, Florida State University, Tallahassee, Florida, USA

^dDepartment of Biomedical Imaging and Image-guided Therapy, Division of Molecular and Gender Imaging, Medical University of Vienna, Vienna, Austria

^eDepartment of Radiology, Breast Imaging Service, Memorial Sloan-Kettering Cancer Center, New York, USA

ABSTRACT

Reducing a graph model is extremely important for the dynamical analysis of large-scale networks. In order to approximate the behavior of such a system it is helpful to be able to simplify the model. In this paper, the graph reduction model is introduced. This method is based on removing edges that close independent cycles in the graph. We apply this novel model reduction paradigm to brain networks, and show the differences between the model approximation error for various brain network graphs ranging from those of healthy controls to those of Alzheimer's patients. The graph simplification for Alzheimer's brain networks yields the smallest approximation error, since the number of independent cycles is smaller than in either the healthy controls or mild cognitive impairment patients.

Keywords: Graph simplification, Cycle removal, Approximation error, Alzheimer, Imaging connectomics

1. INTRODUCTION

Novel mathematical concepts such as graph theoretical techniques can capture the brain connectivity and its topology.¹⁻³ These graph networks are mostly based on Pearson correlation and are used for capturing the structural and/or functional brain connectivity.⁴⁻⁷ From these graphs, new descriptors can be derived in order to quantify induced changes in topology or network organization, or to serve as theory-driven biomarkers to predict dementia at the level of the individual subject.⁸⁻¹¹

Most graph networks applied to dementia research, even for longitudinal data, are static graph networks. These models cannot capture the dynamical processes which govern the time evolution of dementia. Therefore, a new paradigm in dementia research – dynamical graph networks – is required, in order to advance this field and to overcome the obstacles posed by static graph theory in terms of the prediction, evolution, and connectivity changes associated with neurodegenerative diseases.¹²

To address this important issue of analyzing the dynamical behavior, we propose a simplified method which is frequently applied for dynamical systems,¹³⁻¹⁵ and results in a model of lower complexity.

Several methods have been applied to the theory of both dynamical and stochastic systems. Balanced truncation is one such method, and is known as the standard method for model reduction.¹⁶ This method is based on a state-space point of view; employing the canonical observability and controllability Gramian matrices,¹⁷⁻²⁰ and relating to the past input energy (controllability) and future input energy (observability).

* Corresponding Author: Amirhessam Tahmassebi

E-mail: atahmassebi@fsu.edu

URL: <http://www.amirhessam.com>

While for linear systems this procedure is pretty straightforward, for nonlinear systems balancing truncation becomes, in general, somewhat of a complicated task.²¹⁻²³ They are not quite efficient, however, in terms of model reduction for large-scale networks like those found in the human brain. For brain connectivity models, we require a structure preservation between subsystems and at the same time, a network topology-preserving mechanism to provide model reduction. In previous work, we addressed this issue by choosing a technique based on an area aggregation and time-scale modeling for sparse brain networks with densely interconnected hubs and externally sparse interconnections between these hubs.^{24,25} In,²⁶ it was shown that the neurons in the hubs synchronize on the fast time-scale and as aggregated neurons determine the slow dynamics of the neural network. The basic concept of singular perturbation applied in²⁶ has been extensively studied in other neural networks at different time-scales.²⁷⁻³⁶

In this paper, we approximate a brain network using a less complex graph network by removing cycles from the original brain network. The resulting network has nodes that exchange their relative state information with their neighbors. We choose the cycles as independent (not sharing edges with each other) and evaluate the approximation error for dementia networks.

2. MODEL REDUCTION BASED ON CYCLE REMOVAL

2.1 Notation

The trace of the square matrix A is defined as $tr(A)$ and is equal to the sum of its diagonal elements. The cardinality of a set is denoted as \mathcal{E} . The \mathcal{H}_2 -norm of the transfer matrix of a system Σ is defined as $\|\Sigma\|_2$.

2.2 Preliminaries

We consider undirected connected biological networks defined as $\mathcal{G} = (\mathcal{V}, \mathcal{E})$ consisting of a set of nodes $V = \{1, 2, \dots, n\}$ and a set of edges $\mathcal{E} \subset \{i, j | i, j \in \mathcal{V}\}$, the set of all unordered pairs. A graph $\mathcal{G}' = (\mathcal{V}', \mathcal{E}')$ is defined as a subgraph of $\mathcal{G} = (\mathcal{V}, \mathcal{E})$, denoted as $\mathcal{G}' \subset \mathcal{G}$, if $\mathcal{V}' \subset \mathcal{V}$ and $\mathcal{E}' \subset \mathcal{E}$. A spanning tree \mathcal{T} of graph $\mathcal{G} = (\mathcal{V}, \mathcal{E})$ is any connected and cycle-free subgraph of \mathcal{G} with $\mathcal{T} = (\mathcal{V}, \mathcal{E}_t) \subset \mathcal{G}$. If \mathcal{E}_t contains the edges of a spanning tree \mathcal{T} then the set $\mathcal{E}_c = \mathcal{E} \setminus \mathcal{E}_t$ contains the edges in \mathcal{G} which are not in \mathcal{T} . Thus, these edges must close the cycles in \mathcal{G} . The incidence matrix E of \mathcal{G} is given as a $|\mathcal{V}| \times |\mathcal{E}|$ -dimensional matrix with $\mathcal{E}_{ik} = 1$ if node i is the initial node in edge k and is $\mathcal{E}_{ik} = -1$ if its the terminal node, or 0 otherwise. For a given spanning tree \mathcal{T} let E_t denote the columns of the incidence matrix E corresponding to the edges in \mathcal{E}_t and E_c denote the columns corresponding to the edges in \mathcal{E}_c . Renumbering the edges in \mathcal{E} we obtain a new matrix

$$E = [E_t \quad E_c] \quad (1)$$

In³⁷ was a matrix T defined as

$$E_t T = E_c \quad (2)$$

The following two definitions are given for edge-disjoint and correlated cycles.

Definition 1: Two cycles are called edge-disjoint, or independent, if they have no edges in common.

Definition 2: Two cycles are called correlated, or dependent, if they are not edge-disjoint.

Definition 3: The Laplacian matrix L of an undirected graph \mathcal{G} is a positive semi-definite matrix in $R^{n \times n}$ defined based on the incidence matrix to be

$$L = EE^T \quad (3)$$

Under the given formulation, the eigenvalues of L are real and nonnegative, and can be expressed in the following order

$$0 = \lambda_1 < \lambda_2 \leq \dots \leq \lambda_n \quad (4)$$

Definition 4: The edge Laplacian matrix is defined as

$$L_e = E^T E \quad (5)$$

The edge Laplacian is a symmetric positive semi-definite matrix in $R^{|\mathcal{E}| \times |\mathcal{E}|}$ has the same nonzero eigenvalues as the Laplacian.

2.3 Dynamical Approximation Model

We consider a dynamical model $\widehat{\Sigma}$, without an external input and described based on the following equation

$$\Sigma : \quad \dot{x}(t) = -Lx \quad (6)$$

The vector $x \in R^n$ describes the states of the agents and L is the Laplacian matrix of the graph $\mathcal{G} = (\mathcal{V}, \mathcal{E})$. The goal of the model reduction is to approximate the dynamical behavior of the given system by a less complex graph. The strategy that is employed in³⁷ is to remove specific edges in the original graph. The reduced graph $\mathcal{G}' = (\mathcal{V}, \mathcal{E}') \subset \mathcal{G}$ has the same number of nodes as the original graph \mathcal{G} but a subset of edges. The reduced dynamical system $\widehat{\Sigma}'$ is defined as

$$\Sigma' : \quad \dot{x}'(t) = -L'x' \quad (7)$$

with L' being the Laplacian of \mathcal{G}' and $x' \in R^n$. The error of approximation between the two dynamical systems $\widehat{\Sigma}$ and $\widehat{\Sigma}'$ is determined by the \mathcal{H}_2 -norm of the error system. The \mathcal{H}_2 -norm $\|\Sigma - \widehat{\Sigma}'\|_2^2$ represents the energy of the error of the two systems.

In,³⁷ there are two theorems related to removing one edge or k edges, given that determine the absolute approximation error and an upper bound of it.

*Theorem 1.*³⁷ Consider a network Σ consisting of a tree \mathcal{T} and the edge $e \in \bar{\mathcal{E}}_t$ with the graph $\mathcal{G} = (\mathcal{V}, \mathcal{E}_t \cup e)$, such that the graph has one cycle c . The absolute approximation error is then bounded and given as

$$\|\Sigma - \widehat{\Sigma}'\|_2^2 \leq \frac{1}{2} \left(\frac{l(c) - 1}{1 + \frac{\lambda_2}{\lambda_2 + \lambda_n}(l(c) - 1)} + \frac{1}{l(c)} - 1 \right) \quad (8)$$

where λ_2 and λ_n are the smallest nonzero and the largest Laplacian eigenvalues of the spanning tree \mathcal{T} and $l(c)$ is the length of cycle c .

*Theorem 2.*³⁷ Consider a network Σ consisting of a tree \mathcal{T} together with k edges $e_1, e_2, \dots, e_k \in \bar{\mathcal{E}}_t$ with the graph $\mathcal{G} = (\mathcal{V}, \mathcal{E}_t \cup_{j=1}^k \{e_j\})$, such that cycles c_1, c_2, \dots, c_k are independent. The absolute approximation error is then bounded above and given as

$$\|\Sigma - \widehat{\Sigma}'\|_2^2 \leq \frac{1}{2} \sum_{j=1}^k \left(\frac{l(c_j) - 1}{1 + \frac{\lambda_2}{\lambda_2 + \lambda_n}(l(c_j) - 1)} + \frac{1}{l(c_j)} - 1 \right) \quad (9)$$

where λ_2 and λ_n are the smallest nonzero and the largest Laplacian eigenvalues of the spanning tree \mathcal{T} and $l(c)$ is the length of cycle c .

If all the cycles are independent, then the approximation error equals the sum of the errors bounds corresponding to the removal of independent edges.

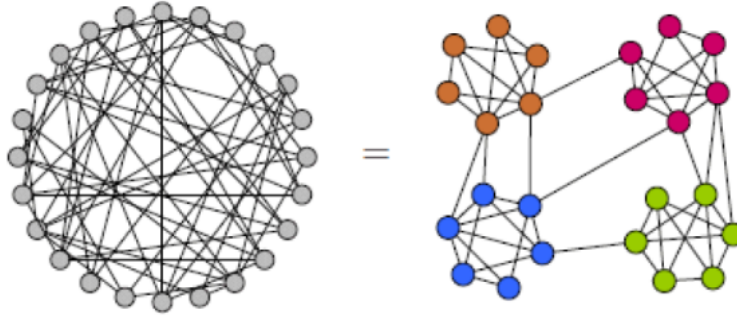


Figure 1. Graphs excel at hiding their structure. Graph clustering aims at revealing their structure.

3. MODEL REDUCTION BASED ON AREA AGGREGATION

Graph networks can exhibit a structure of dense clustered areas, but may have sparse connections between these areas as shown in Figure 3.

They can be dynamically approximated by a two-time scale system, where the neurons within the same area synchronize on the fast time-scale because the dense within-area connections drive the nodes of the given area quickly to reach an equilibrium.

At the same time, the exchange between the areas is based on sparse connections, and can be described at a slow time-scale. This coupled dynamics leads to a reduced-order model which describes the long-term behavior of the overall network.

The large-scale brain network is viewed as an interconnected graph with links between the areas of the brain which are viewed as nodes. Two main parameters describe such a network:²⁶ the node parameter d and the area parameter δ . The node parameter is given to be:

$$d = \frac{c^E}{c^I} \ll 1 \quad (10)$$

where c^E are the densest external links over all nodes and areas and c^I are sparsest internal links over all existing areas. d needs to be a small number. The area parameter is given as

$$\delta = \frac{\gamma^E}{mc^I} \ll 1 \quad (11)$$

where γ^E are the densest external links over all areas and m is the minimal number of nodes found in an area.

In order to obtain a reduced-model approximation, we view the large-scale graph as a structured representations with dense areas (clusters) and sparse interconnections between these areas.²⁶

4. APPLICATION TO STRUCTURAL BRAIN NETWORKS IN DEMENTIA

We apply the theoretical results for graph simplification on structural (MRI) connectivity graphs³⁸ for control (CN), mild cognitive impairment (MCI) and Alzheimer's disease (AD) subjects. For the structural data, the connections in the graph show the inter-regional covariation of gray matter volumes in different areas. In,³⁸ only 42 out of the 116 were considered from the AAL in the frontal, parietal, occipital and temporal lobes. The nodes in the graphs depict the regions, while the edges show if a connection exists between these regions or not.

The structural graphs and the removed edges are shown in Figure 4.

In Table 1, the different approximation errors are given for the three groups. The lowest approximation error is for Alzheimer's patients. This is because the graph has less independent cycles than both the controls and

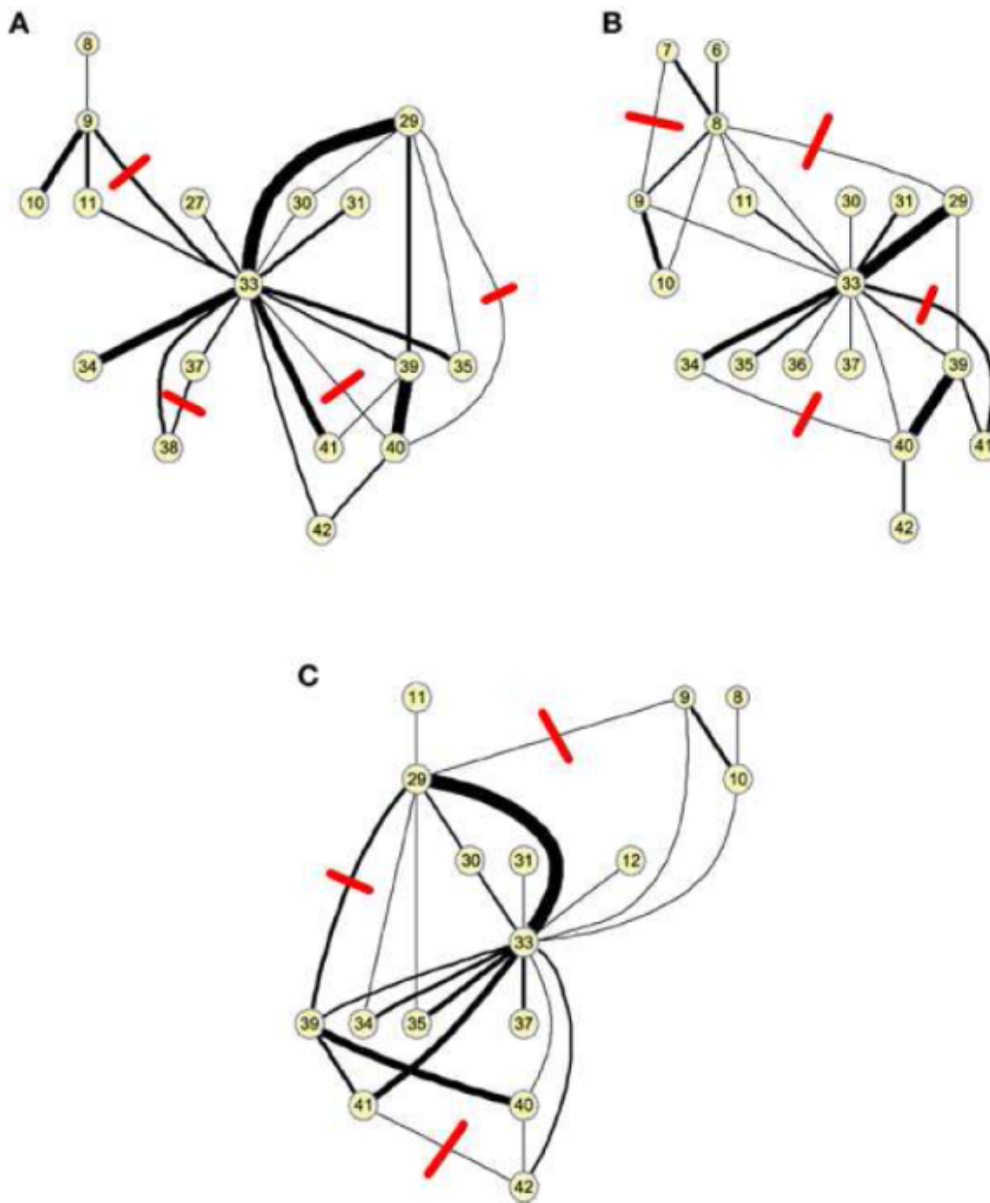


Figure 2. Controllable structural brain networks with the leader set for (A) controls, (B) MCI, and (C) AD.

MCI. For controls and MCI, the error is almost similar as is the number of independent cycles. The results suggest that the Alzheimer's network is best approximated by a reduced graph.

We also applied the area aggregation method to the structural brain networks, and were able to determine two distinct aggregation areas for healthy controls and MCI. For Alzheimer's, however, the theoretical assumptions were not fulfilled²⁴ and thus we could not determine the parameters. The area aggregation parameters determined in²⁴ are given in Table 2. The controls show smaller node and area parameters than the MCIs.

Both model reduction methods – the graph simplification based on cycle removal and the area aggregation methods – show that Alzheimer's networks play an "outlier" role in the graph dynamics, while healthy controls and MCI exhibit more similar dynamical properties.

Subjects	Number of independent cycles	Approximation error
Controls	4	2.26
MCI	4	2.28
Alzheimer's	3	1.68

Table 1. Approximation error resulting from graph simplification for structural brain networks.

Subject	Node Parameter d	Area Parameter δ
CN	$d_{ave} = \frac{1}{5}$	$\delta = \frac{1}{5}$
MCI	$d_{ave} = \frac{2}{3}$	$\delta = \frac{2}{3}$
AD	-	-

Table 2. Area aggregation parameters structural connectivity graphs.³⁸

5. CONCLUSION AND DISCUSSION

This paper presents a new method of reducing large-scale biological graph networks, and gives upper bounds for the absolute approximation error when these biological networks are approximated by removing cycles from the original network. The results for dementia brain networks reveal that their best approximation is given based on graph simplification for Alzheimer's networks, since there are less independent cycles compared to controls and MCIs. Additionally, a comparison with a second graph approximation method based on area aggregation is given.

Acknowledgement

This research was supported in part by Fulbright.

REFERENCES

- [1] Fornito, A., Zalesky, A., Pantelis, C., and Bullmore, E., “Schizophrenia, neuroimaging and connectomics,” *Neuroimage* **62**, 2296–2314 (1 2012).
- [2] Giessing, C. and Thiel, C., “Pro-cognitive drug effects modulate functional brain network organization,” *Frontiers in Behavioral Neuroscience* **6**, 1–9 (1 2012).
- [3] Zeng, L., Shen, H., Liu, L., Wang, L., Li, B., Fang, P., Zhou, Z., Li, Y., and Hu, D., “Identifying major depression using whole-brain functional connectivity: a multivariate pattern analysis,” *Brain* **1498**, 1498–1507 (4 2012).
- [4] Hartman, D., Hlinka, J., Palus, M., Mantini, D., and Corbetta, M., “The role of nonlinearity in computing graph-theoretical properties of resting-state functional magnetic resonance imaging brain networks,” *Chaos* **21**, 013119 (1 2011).
- [5] Alexander-Bloch, A., Vertes, P., Stidd, R., Lalonde, F., Clasen, L., Rapoport, J., Giedd, J., Bullmore, E., and Gogtay, N., “The anatomical distance of functional connections predicts brain network topology in health and schizophrenia,” *Cerebral Cortex* **23**, 127–138 (1 2013).
- [6] Nigri, A., Ferraro, S., D’incerti, L., Critchley, H., Bruzzone, M., and Minati, L., “Connectivity of the amygdala, piriform, and orbitofrontal cortex during olfactory stimulation: a functional mri study,” *NeuroReport* **24**, 171–175 (1 2013).
- [7] Wheland, D., Joshi, A., McMahan, K., Hansell, N., Martin, N., Wright, M., Thomson, P., Shattuk, D., and Leahy, R., “Robust identification of partial-correlation based networks with applications to cortical thickness data,” *9th IEEE International Symposium on Biomedical Imaging (ISBI)* **3**, 1551–1554 (5 2012).
- [8] Tahmassebi, A., Pinker-Domenig, K., Wengert, G., Lobbes, M., Stadlbauer, A., Romero, F. J., Morales, D. P., Castillo, E., Garcia, A., Botella, G., et al., “Dynamical graph theory networks techniques for the analysis of sparse connectivity networks in dementia,” in [*Smart Biomedical and Physiological Sensor Technology XIV*], **10216**, 1021609, International Society for Optics and Photonics (2017).
- [9] Tahmassebi, A., “ideeple: Deep learning in a flash,” in [*Disruptive Technologies in Information Sciences*], **10652**, 106520S, International Society for Optics and Photonics (2018).
- [10] Tahmassebi, A., Pinker-Domenig, K., Wengert, G., Lobbes, M., Stadlbauer, A., Wildburger, N. C., Romero, F. J., Morales, D. P., Castillo, E., Garcia, A., et al., “The driving regulators of the connectivity protein network of brain malignancies,” in [*Smart Biomedical and Physiological Sensor Technology XIV*], **10216**, 1021605, International Society for Optics and Photonics (2017).
- [11] Tahmassebi, A., Amani, A. M., Pinker-Domenig, K., and Meyer-Baese, A., “Determining disease evolution driver nodes in dementia networks,” in [*Medical Imaging 2018: Biomedical Applications in Molecular, Structural, and Functional Imaging*], **10578**, 1057829, International Society for Optics and Photonics (2018).
- [12] Tang, Y., Wang, Z., Gao, H., Swift, S., and Kurths, J., “A constrained evolutionary computation method for detecting controlling regions of cortical networks,” *IEEE/ACM Transactions on computational biology and bioinformatics* **9**, 1569–1581 (1 2012).
- [13] Utkin, V. I., [*Sliding Modes in Optimization and Control*], Springer Verlag (1992).
- [14] Cao, W.-J. and Xu, J.-X., “Nonlinear integral-type sliding surface for both matched and unmatched uncertain systems,” *IEEE Transactions on Automatic Control* , 1355–1360 (August 2004).
- [15] Mohebbi, B., “Characterization of the common mode features of a 3-phase full-bridge inverter using frequency domain approaches,” (2016).
- [16] Moore, B., “Principal component analysis in linear systems: controllability, observability and model reduction,” *IEEE Transactions on Automatic Control* , 17–32 (January 1981).
- [17] Meyer-Bäse, A., Theis, F., and Conrad, C., “Uncertain gene regulatory networks simplified by gramian-based approach,” *International Conference on Bioinformatics and Computational Biology 2011* , In print (4 2011).
- [18] Lall, S., Marsden, J., and Glavaski, S., “A subspace approach to balanced truncation for model reduction of nonlinear control systems,” *Int. Journal of Robust and Nonlinear Control* (February 2002).
- [19] Scherpen, J., “Balancing for nonlinear systems,” *Systems and Control Letters* , 143–153 (March 1993).

- [20] Mohebalı, B., Tahmassebi, A., Gandomi, A. H., Meyer-Baese, A., and Foo, S. Y., “A scalable communication abstraction framework for internet of things applications using raspberry pi,” in [*Disruptive Technologies in Information Sciences*], **10652**, 1065205, International Society for Optics and Photonics (2018).
- [21] Meyer-Bäse, A., “Gene regulatory networks simplified by nonlinear balanced truncation,” *SPIE Proceedings Series* **6979**, 69790C (4 2008).
- [22] Meyer-Baese, A. and Theis, F., “Gene regulatory networks simplified by nonlinear balanced truncation,” *SPIE Symposium Computational Intelligence* **6979**, 6979C (7 2008).
- [23] Graber, L., Mohebalı, B., Bosworth, M., Steurer, M., Card, A., Rahmani, M., and Mazzola, M., “How scattering parameters can benefit the development of all-electric ships,” in [*2015 IEEE Electric Ship Technologies Symposium (ESTS)*], 353–357, IEEE (2015).
- [24] Meyer-Baese, A., Roberts, R., Illan, I., Meyer-Baese, U., Lobbes, M., Stadlbauer, A., and Pinker-Domenig, K., “Dynamical graph theory networks methods for the analysis of sparse functional connectivity networks and for determining pinning observability in brain networks,” *Frontiers in Computational Neuroscience* <https://doi.org/10.3389/fncom.2017.00087> (1 2017).
- [25] Meyer-Baese, A., Amani, A. M., Meyer-Baese, U., Foo, S., Stadlbauer, A., and Yu, W., “Pinning observability of competitive neural networks with different time constants,” *Neurocomputing* **In press** (1 2018).
- [26] Chow, J. H. and Kokotovic, P., “Time scale modeling of sparse dynamic networks,” *IEEE Transaction on Automatic Control* **30**, 714–722 (3 1985).
- [27] Meyer-Baese, A., Roberts, R., and Thuemmler, V., “Local uniform stability of competitive neural networks with different time-scales under vanishing perturbations,” *Neurocomputing* **73**, 770–775 (4 2010).
- [28] Meyer-Baese, A., Roberts, R., and Yu, H., “Robust stability analysis of competitive neural networks with different time-scales under perturbations,” *Neurocomputing* **71**, 417–420 (11 2007).
- [29] Meyer-Baese, A. and Pilyugin, S., “Global asymptotic stability of a class of dynamical neural networks,” *International Journal of Neural Systems* , 47–53 (2 2003).
- [30] Meyer-Baese, A., Pilyugin, S., and Chen, Y., “Global exponential stability of competitive neural networks with different time scales,” *IEEE Transactions on Neural Networks* , 716–719 (2 2003).
- [31] Meyer-Baese, A. and Pilyugin, S., “Flow invariance for competitive multi-modal neural networks,” *International Joint Conference on Neural Networks* , 3101–3105 (7 2003).
- [32] Meyer-Baese, A., Pilyugin, S., and Wisniewski, A., “Stability analysis of self-organizing multi-time scale neural networks,” *International Joint Conference on Neural Networks* (4 2004).
- [33] Meyer-Baese, A., Pilyugin, S., Wisniewski, A., and Foo, S., “Local exponential stability of competitive neural networks with different time-scales,” *Engineering Application of Artificial Intelligence* , 227–232 (9 2004).
- [34] Meyer-Baese, A. and Thummler, V., “Local and global stability analysis of an unsupervised competitive neural network,” *IEEE Transactions on Neural Networks* **19**, 346–351 (5 2008).
- [35] Mohebalı, B., Breslend, P., Graber, L., and Steurer, M., “Validation of a scattering parameter based model of a power cable for shipboard grounding studies,” in [*ASNE Electric Machines Symposium (EMTS)*], **201**, 28–29 (2014).
- [36] Kia, M., Rezayieh, K. R., and Mohebalı, B., “A novel position sensor in mobile robots motion control,” (2012).
- [37] Jongsma, H. J., Trentelman, H. L., and Camlibel, M. K., “Model reduction of consensus networks by graph simplification,” *Proceedings of the 54th IEEE Conference on Decision and Control* **4**, 5340–5345 (1 2015).
- [38] Ortiz, A., Munilla, J., Alvarez-Illan, I., Gorriz, M., and Ramirez, J., “Exploratory graphical models of functional and structural connectivity patterns for alzheimer’s disease diagnosis,” *Frontiers in Computational Neuroscience* <http://dx.doi.org/10.3389/fncom.2015.00132> (1 2015).